Supporting Information

Green-Light-Selective Organic Photodiodes with High Detectivity for CMOS Color Image Sensors

Younhee Lim[1,], Sungyoung Yun[1], Daiki Minami[2], Taejin Choi[1], Hyesung Choi[1], Jisoo Shin[1], Chul-Joon Heo[1], Dong-Seok Leem[1], Tadao Yagi[3,*], Kyung-Bae Park[1] and Sunghan Kim[1]*

[1] Organic Materials Laboratory, Samsung Advanced Institute of Technology (SAIT), Samsung Electronics, Co. Ltd., 130, Samsung-ro, Yeongtong-gu, Suwon-si, Gyeonggi-do 16678, Republic of Korea

[2] Data & Information Technology (DIT) Center, Samsung Electronics, Co. Ltd, 1, Samsungjeonja-ro, Hwaseong-si, Gyeonggi-do 18448, Korea

[3] MD-2 Lab, Samsung R&D Institute Japan-Yokohama (SRJ-Y), Samsung Electronics, Co. Ltd., 2-7, Sugasawa-cho, Tsurumi-ku, Yokohama 230-0027, Japan

*E-mail: younhee.lim@samsung.com (Younhee Lim)

*E-mail: t.yagi@samsung.com (Tadao Yagi)

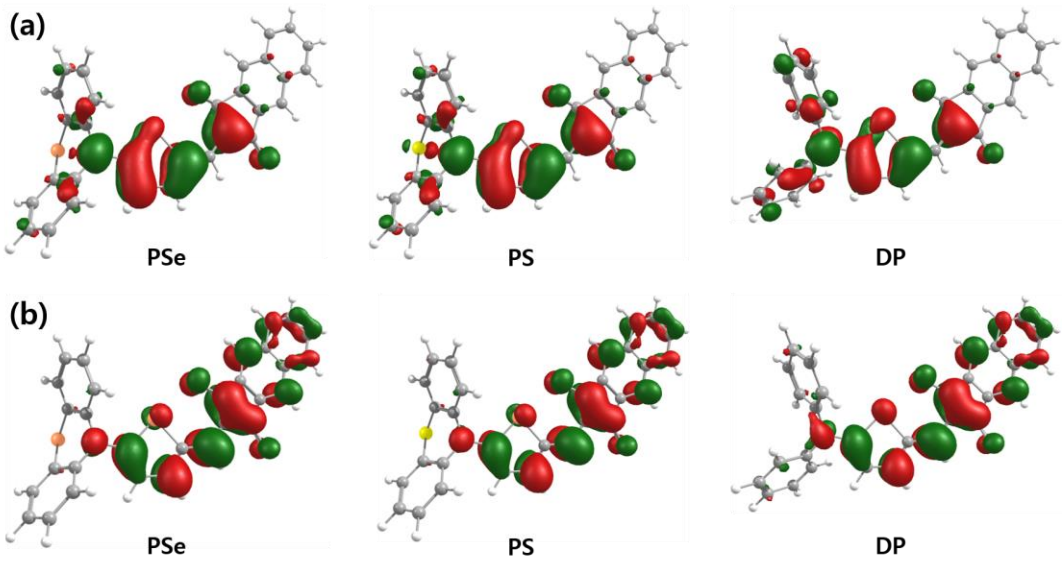

Figure S1. Density functional theory (DFT)-predicted frontier molecular orbitals of the molecules. (a) HOMO and (b) LUMO molecular orbitals.

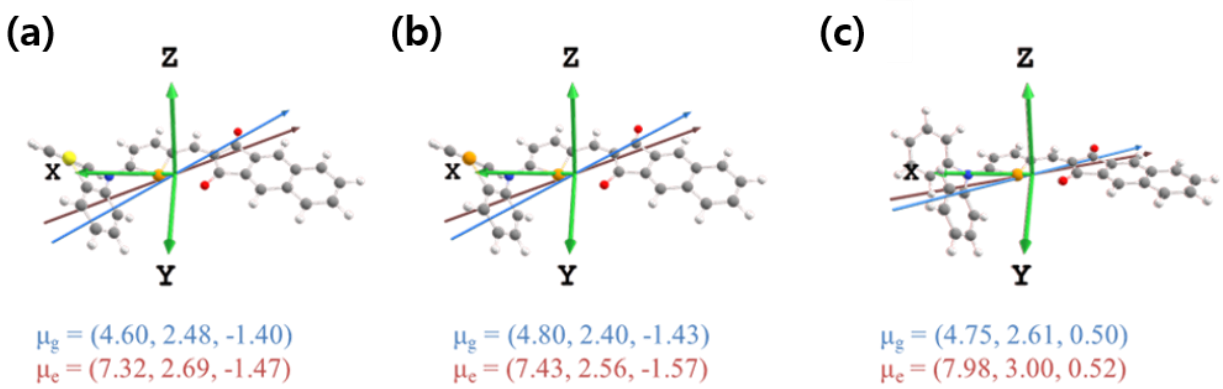

Figure S2. Calculated dipole moment vectors for the ground and excited states of (a) PSe, (b) PS, and (c) DP molecules. Blue and red arrows represent the ground and excited state dipole moments, respectively.

Table S1. TD-DFT calculated absorption transition obtained from DP, PS, and PSe.

Molecule	S0 → S1	Energy gap (eV)	*f*
PSe	HOMO → LUMO 0.69824	2.68	0.997
PS	HOMO → LUMO 0.69888	2.67	1.001
DP	HOMO → LUMO 0.69743	2.56	0.963

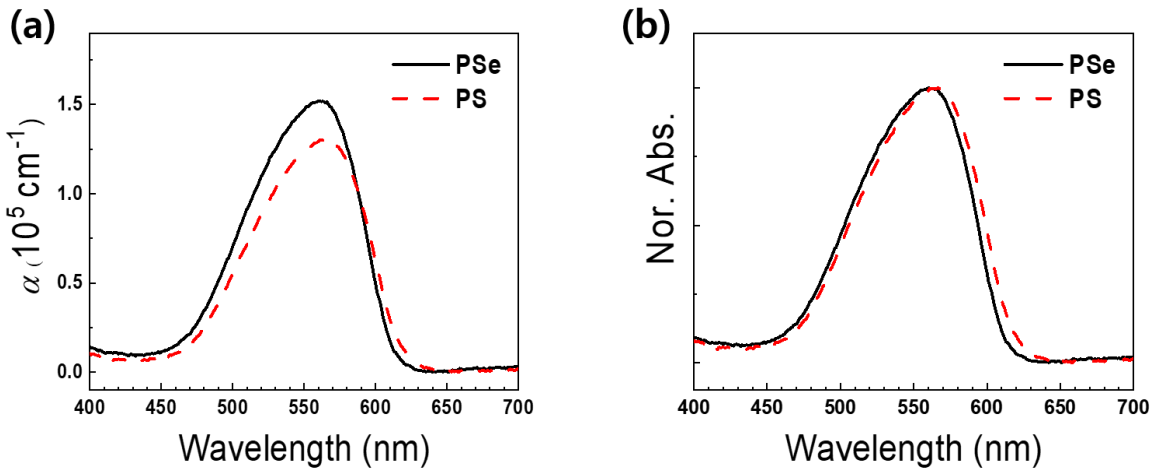

Figure S3. (a) Visible light absorption spectra and (b) normalized absorption spectra of the films of PSe (black solid line) and PS (red dashed line).

Table S2. Mixing energies of the p- and n-type mixtures.

	E_{mix} (kcal/mol)	E_{nn} (kcal/mol)	E_{pn} (kcal/mol)	E_{pp} (kcal/mol)	Z_{nn}	Z_{np}	Z_{pn}	Z_{pp}
PSe	0.69	-7.42	-11.58	-16.03	5.51	4.95	6.19	5.58
PS	3.26	-7.42	-11.56	-16.90	5.51	4.95	6.18	5.58
DP	5.54	-7.42	-10.65	-15.91	5.51	4.94	6.19	5.58

The mixing energies (E_{mix}) were calculated from the binding energies (Enn, Epn, and Epp) and coordination numbers (Z_{nn}, Z_{np}, Z_{pn}, and Z_{pp}) between the p- and n-type molecules using Equation S1.

$$E_{mix} = \frac{1}{2}\left(Z_{pn}E_{pn} + Z_{np}E_{pn} - Z_{nn}E_{nn} - Z_{pp}E_{pp}\right) \qquad \text{eq. S1}$$

The binding energies (E_{nn}, E_{pn}, and E_{pp}) were calculated by Monte Carlo (MC) methods using blend module of BIOVIA Materials studio (Dassault sytems, San Diego). In this calculations, the stable configurations of dimers of p-p, p-n and n-n were generated by the MC steps and the inter-molecular interaction energies were calculated using the universal force-field which is a classical force field for molecular dynamics simulations. The intermolecular interaction energies for stable configurations of dimers generated through 2,000,000 MC-steps were averaged to obtain the binding energies for each pairs. The packing structures of coordinating molecules were obtained by the 10,000 MC-steps to calculate the coordination numbers (Z_{nn}, Z_{np}, Z_{pn}, and Z_{pp}) for each molecular pairs. The mixing energies were calculated from the binding energies and coordination numbers.

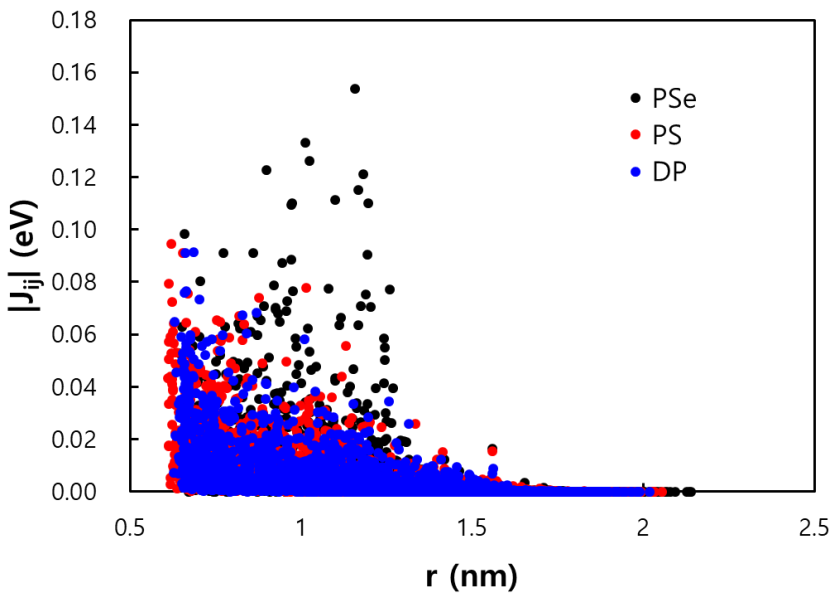

Figure S4. Transfer integrals of the HOMO for p- and n-type molecular pairs with a cut-off distance of 2.5 nm in the morphologies of the bulk heterojunctions consisting of p- and n-type molecules (sampling numbers for PSe, PS, and DP mixtures are 2428, 2428, and 2674, respectively). All calculations are performed using Deposit and QuantumPatch at B3LYP/Def2-SVP level (Nanomatch GmbH, Germany).

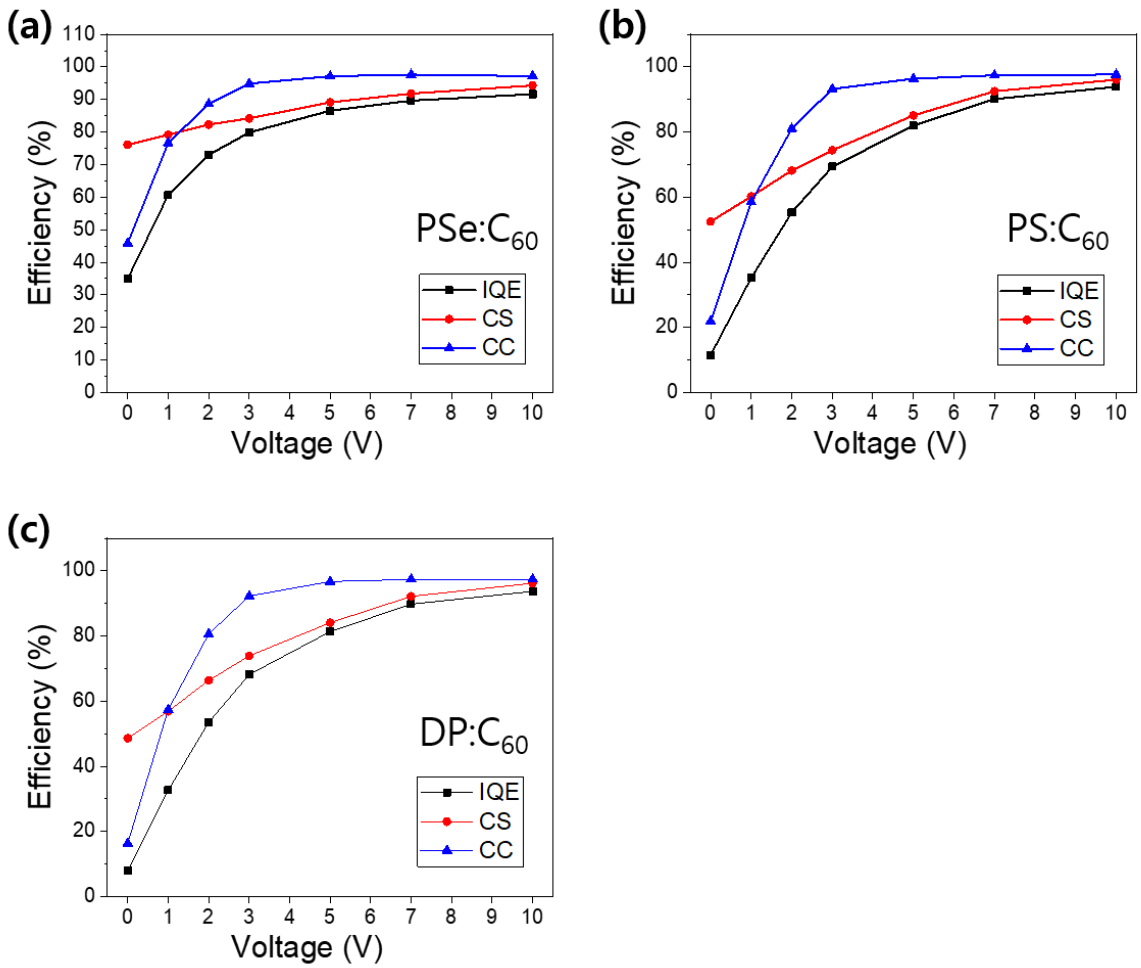

Figure S5. The internal quantum efficiency (IQE, black), charge separation efficiency (CS, η_{cs}, red), and charge collection efficiency (CC, η_{cc}, blue) changes as a function of the electric field for (a) PSe:C_{60}, (b) PS:C_{60}, and (c) DP:C_{60}-based OPDs. The charge collection efficiency was evaluated by using the expression EQE = absorptance (η_A) × IQE = $\eta_A \times \eta_{cs} \times \eta_{cc}$.

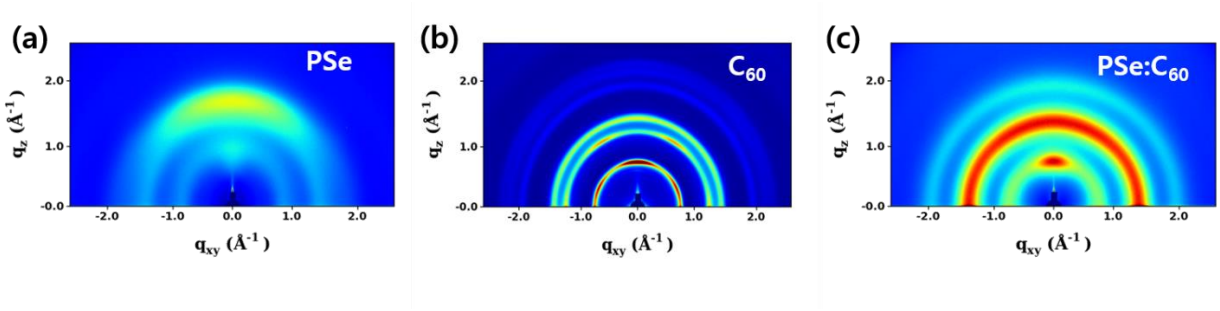

Figure S6. GIWAXS spectra of (a) PSe, (b) C60, and (c) PSe:C60 thin films.

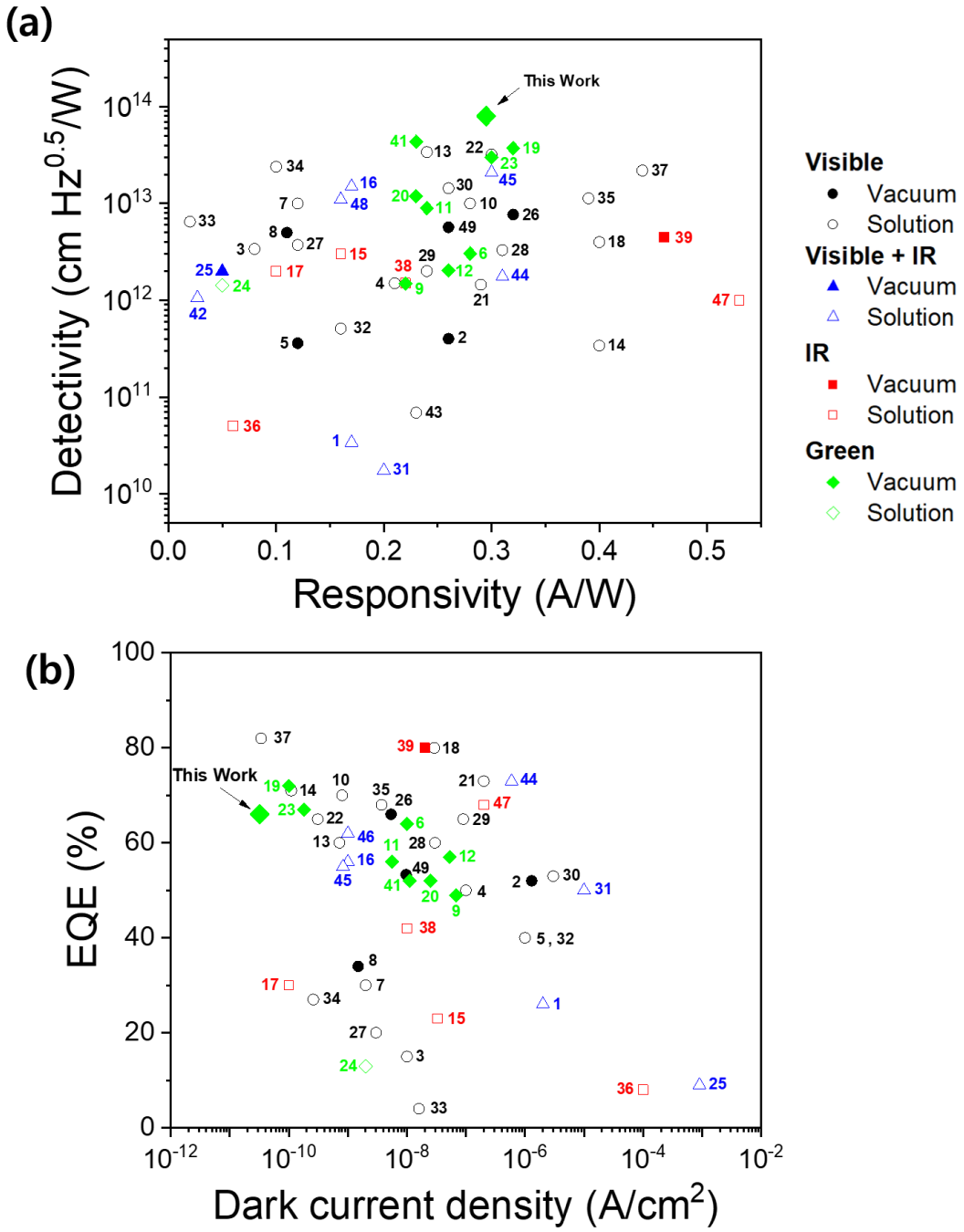

Figure S7. The state-of-the-art of organic photodiodes (OPDs). Comparison of (a) specific detectivity, responsivity, (b) EQE, and dark current for vacuum and solution processed OPDs published in the literature. Numbers indicate references.[S1-S49]

References

(S1) Gong, X.; Tong, M.; Xia, Y.; Cai, W.; Moon, J. S.; Cao, Y.; Yu, G.; Shieh, C.-L.; Nilsson, B.; Heeger, A. J. High-Detectivity Polymer Photodetectors with Spectral Response from 300 Nm to 1450 Nm. *Science* **2009**, *325* (5948), 1665–1667. https://doi.org/10.1126/science.1176706.

(S2) Higashi, Y.; Kim, K.-S.; Jeon, H.-G.; Ichikawa, M. Enhancing Spectral Contrast in Organic Red-Light Photodetectors Based on a Light-Absorbing and Exciton-Blocking Layered System. *J. Appl. Phys.* **2010**, *108* (3), 034502. https://doi.org/10.1063/1.3466766.

(S3) Binda, M.; Iacchetti, A.; Natali, D.; Beverina, L.; Sassi, M.; Sampietro, M. High Detectivity Squaraine-Based near Infrared Photodetector with NA/Cm2 Dark Current. *Appl. Phys. Lett.* **2011**, *98* (7), 073303. https://doi.org/10.1063/1.3553767.

(S4) Azzellino, G.; Grimoldi, A.; Binda, M.; Caironi, M.; Natali, D.; Sampietro, M. Fully Inkjet-Printed Organic Photodetectors with High Quantum Yield. *Adv. Mater.* **2013**, *25* (47), 6829–6833. https://doi.org/10.1002/adma.201303473.

(S5) Guo, F.; Xiao, Z.; Huang, J. Fullerene Photodetectors with a Linear Dynamic Range of 90 DB Enabled by a Cross-Linkable Buffer Layer. *Adv. Opt. Mater.* **2013**, *1* (4), 289–294. https://doi.org/10.1002/adom.201200071.

(S6) Leem, D.-S.; Lee, K.-H.; Park, K.-B.; Lim, S.-J.; Kim, K.-S.; Wan Jin, Y.; Lee, S. Low Dark Current Small Molecule Organic Photodetectors with Selective Response to Green Light. *Appl. Phys. Lett.* **2013**, *103* (4), 043305. https://doi.org/10.1063/1.4816502.

(S7) Saracco, E.; Bouthinon, B.; Verilhac, J.-M.; Celle, C.; Chevalier, N.; Mariolle, D.; Dhez, O.; Simonato, J.-P. Work Function Tuning for High-Performance Solution-Processed Organic Photodetectors with Inverted Structure. *Adv. Mater.* **2013**, *25* (45), 6534–6538. https://doi.org/10.1002/adma.201302338.

(S8) Yang, D.; Zhou, X.; Ma, D. Fast Response Organic Photodetectors with High Detectivity Based on Rubrene and C60. *Org. Electron.* **2013**, *14* (11), 3019–3023. https://doi.org/10.1016/j.orgel.2013.08.027.

(S9) Lee, K.-H.; Leem, D.-S.; Castrucci, J. S.; Park, K.-B.; Bulliard, X.; Kim, K.-S.; Jin, Y. W.; Lee, S.; Bender, T. P.; Park, S. Y. Green-Sensitive Organic Photodetectors with High Sensitivity and Spectral Selectivity Using Subphthalocyanine Derivatives. *ACS Appl. Mater. Interfaces* **2013**, *5* (24), 13089–13095. https://doi.org/10.1021/am404122v.

(S10) Armin, A.; Hambsch, M.; Kim, I. K.; Burn, P. L.; Meredith, P.; Namdas, E. B. Thick Junction Broadband Organic Photodiodes. *Laser Photonics Rev.* **2014**, *8* (6), 924–932. https://doi.org/10.1002/lpor.201400081.

(S11) Leem, D.-S.; Lee, K.-H.; Kwon, Y.-N.; Yun, D.-J.; Park, K.-B.; Lim, S.-J.; Kim, K.-S.; Jin, Y. W.; Lee, S. Low Dark Current Inverted Organic Photodetectors Employing MoOx:Al Cathode Interlayer. *Org. Electron.* **2015**, *24*, 176–181. https://doi.org/10.1016/j.orgel.2015.05.044.

(S12) Lim, S.-J.; Leem, D.-S.; Park, K.-B.; Kim, K.-S.; Sul, S.; Na, K.; Lee, G. H.; Heo, C.-J.; Lee, K.-H.; Bulliard, X.; Satoh, R.-I.; Yagi, T.; Ro, T.; Im, D.; Jung, J.; Lee, M.; Lee, T.-Y.; Han, M. G.; Jin, Y. W.; Lee, S. Organic-on-Silicon Complementary Metal–Oxide–Semiconductor Colour Image Sensors. *Sci. Rep.* **2015**, *5* (1), 7708. https://doi.org/10.1038/srep07708.

(S13) Pierre, A.; Deckman, I.; Lechêne, P. B.; Arias, A. C. High Detectivity All-Printed Organic Photodiodes. *Adv. Mater.* **2015**, *27* (41), 6411–6417. https://doi.org/10.1002/adma.201502238.

(S14) Kim, I. K.; Pal, B. N.; Ullah, M.; Burn, P. L.; Lo, S.-C.; Meredith, P.; Namdas, E. B. High-Performance, Solution-Processed Non-Polymeric Organic Photodiodes. *Adv. Opt. Mater.* **2015**, *3* (1), 50–56. https://doi.org/10.1002/adom.201400385.

(S15) Zhang, H.; Jenatsch, S.; De Jonghe, J.; Nüesch, F.; Steim, R.; Véron, A. C.; Hany, R. Transparent Organic Photodetector Using a Near-Infrared Absorbing Cyanine Dye. *Sci. Rep.* **2015**, *5* (1), 9439. https://doi.org/10.1038/srep09439.

(S16) Zhou, X.; Yang, D.; Ma, D. Extremely Low Dark Current, High Responsivity, All-Polymer Photodetectors with Spectral Response from 300 Nm to 1000 Nm. *Adv. Opt. Mater.* **2015**, *3* (11), 1570–1576. https://doi.org/10.1002/adom.201500224.

(S17) Armin, A.; Jansen-van Vuuren, R. D.; Kopidakis, N.; Burn, P. L.; Meredith, P. Narrowband Light Detection via Internal Quantum Efficiency Manipulation of Organic Photodiodes. *Nat. Commun.* **2015**, *6* (1), 6343. https://doi.org/10.1038/ncomms7343.

(S18) Kim, I. K.; Li, X.; Ullah, M.; Shaw, P. E.; Wawrzinek, R.; Namdas, E. B.; Lo, S.-C. High-Performance, Fullerene-Free Organic Photodiodes Based on a Solution-Processable Indigo. *Adv. Mater.* **2015**, *27* (41), 6390–6395. https://doi.org/10.1002/adma.201502936.

(S19) Han, M. G.; Park, K.-B.; Bulliard, X.; Lee, G. H.; Yun, S.; Leem, D.-S.; Heo, C.-J.; Yagi, T.; Sakurai, R.; Ro, T.; Lim, S.-J.; Sul, S.; Na, K.; Ahn, J.; Jin, Y. W.; Lee, S. Narrow-Band Organic Photodiodes for High-Resolution Imaging. *ACS Appl. Mater. Interfaces* **2016**, *8* (39), 26143–26151. https://doi.org/10.1021/acsami.6b07735.

(S20) Bulliard, X.; Jin, Y. W.; Lee, G. H.; Yun, S.; Leem, D.-S.; Ro, T.; Park, K.-B.; Heo, C.-J.; Satoh, R.-I.; Yagi, T.; Choi, Y. S.; Lim, S.-J.; Lee, S. Dipolar Donor–Acceptor Molecules in the Cyanine Limit for High Efficiency Green-Light-Selective Organic Photodiodes. *J. Mater. Chem. C* **2016**, *4* (5), 1117–1125. https://doi.org/10.1039/C5TC03567H.

(S21) Grimoldi, A.; Colella, L.; La Monaca, L.; Azzellino, G.; Caironi, M.; Bertarelli, C.; Natali, D.; Sampietro, M. Inkjet Printed Polymeric Electron Blocking and Surface Energy Modifying Layer for Low Dark Current Organic Photodetectors. *Org. Electron.* **2016**, *36*, 29–34. https://doi.org/10.1016/j.orgel.2016.05.021.

(S22) Kielar, M.; Dhez, O.; Pecastaings, G.; Curutchet, A.; Hirsch, L. Long-Term Stable Organic Photodetectors with Ultra Low Dark Currents for High Detectivity Applications. *Sci. Rep.* **2016**, *6* (1), 39201. https://doi.org/10.1038/srep39201.

(S23) Heo, S.; Lee, J.; Kim, S. H.; Yun, D.-J.; Park, J.-B.; Kim, K.; Kim, N.; Kim, Y.; Lee, D.; Kim, K.-S.; Kang, H. J. Device Performance Enhancement via a Si-Rich Silicon Oxynitride Buffer Layer for the Organic Photodetecting Device. *Sci. Rep.* **2017**, *7* (1), 1516. https://doi.org/10.1038/s41598-017-01653-z.

(S24) Sung, M. J.; Kim, K.; Kwon, S.-K.; Kim, Y.-H.; Chung, D. S. Phenanthro[110,9,8-Cdefg]Carbazole-Thiophene, Donor–Donor Copolymer for Narrow Band Green-Selective Organic Photodiode. *J. Phys. Chem. C* **2017**, *121* (29), 15931–15936. https://doi.org/10.1021/acs.jpcc.7b04793.

(S25) Wu, Z.; Yao, W.; London, A. E.; Azoulay, J. D.; Ng, T. N. Temperature-Dependent Detectivity of Near-Infrared Organic Bulk Heterojunction Photodiodes. *ACS Appl. Mater. Interfaces* **2017**, *9* (2), 1654–1660. https://doi.org/10.1021/acsami.6b12162.

(S26) Li, W.; Guo, H.; Wang, Z.; Dong, G. Narrowband Organic Photodiodes Based on Green Light Sensitive Squarylium. *J. Phys. Chem. C* **2017**, *121* (28), 15333–15338. https://doi.org/10.1021/acs.jpcc.7b03412.

(S27) Nie, R.; Deng, X.; Feng, L.; Hu, G.; Wang, Y.; Yu, G.; Xu, J. Highly Sensitive and Broadband Organic Photodetectors with Fast Speed Gain and Large Linear Dynamic Range at Low Forward Bias. *Small* **2017**, *13* (24), 1603260. https://doi.org/10.1002/smll.201603260.

(S28) Yoon, S.; Cho, J.; Sim, K. M.; Ha, J.; Chung, D. S. Low Dark Current Inverted Organic Photodiodes Using Anionic Polyelectrolyte as a Cathode Interlayer. *Appl. Phys. Lett.* **2017**, *110* (8), 083301. https://doi.org/10.1063/1.4977025.

(S29) Eckstein, R.; Strobel, N.; Rödlmeier, T.; Glaser, K.; Lemmer, U.; Hernandez-Sosa, G. Fully Digitally Printed Image Sensor Based on Organic Photodiodes. *Adv. Opt. Mater.* **2018**, *6* (5), 1701108. https://doi.org/10.1002/adom.201701108.

(S30) Benavides, C. M.; Murto, P.; Chochos, C. L.; Gregoriou, V. G.; Avgeropoulos, A.; Xu, X.; Bini, K.; Sharma, A.; Andersson, M. R.; Schmidt, O.; Brabec, C. J.; Wang, E.; Tedde, S. F. High-Performance Organic Photodetectors from a High-Bandgap Indacenodithiophene-Based π-Conjugated Donor–Acceptor Polymer. *ACS Appl. Mater. Interfaces* **2018**, *10* (15), 12937–12946. https://doi.org/10.1021/acsami.8b03824.

(S31) Strobel, N.; Seiberlich, M.; Rödlmeier, T.; Lemmer, U.; Hernandez-Sosa, G. Non-Fullerene-Based Printed Organic Photodiodes with High Responsivity and Megahertz Detection Speed. *ACS Appl. Mater. Interfaces* **2018**, *10* (49), 42733–42739. https://doi.org/10.1021/acsami.8b16018.

(S32) Strobel, N.; Eckstein, R.; Lehr, J.; Lemmer, U.; Hernandez-Sosa, G. Semiconductor:Insulator Blends for Speed Enhancement in Organic Photodiodes. *Adv. Electron. Mater.* **2018**, *4* (10), 1700345. https://doi.org/10.1002/aelm.201700345.

(S33) Kim, S.-K.; Park, S.; Son, H. J.; Chung, D. S. Synthetic Approach To Achieve a Thin-Film Red-Selective Polymer Photodiode: Difluorobenzothiadiazole-Based Donor–Acceptor Polymer with Enhanced Space Charge Carriers. *Macromolecules* **2018**, *51* (20), 8241–8247. https://doi.org/10.1021/acs.macromol.8b01751.

(S34) Kim, K.; Sim, K. M.; Yoon, S.; Jang, M. S.; Chung, D. S. Defect Restoration of Low-Temperature Sol-Gel-Derived ZnO via Sulfur Doping for Advancing Polymeric Schottky Photodiodes. *Adv. Funct. Mater.* **2018**, *28* (30), 1802582. https://doi.org/10.1002/adfm.201802582.

(S35) Park, J. B.; Ha, J.-W.; Yoon, S. C.; Lee, C.; Jung, I. H.; Hwang, D.-H. Visible-Light-Responsive High-Detectivity Organic Photodetectors with a 1 Mm Thick Active Layer. *ACS Appl. Mater. Interfaces* **2018**, *10* (44), 38294–38301. https://doi.org/10.1021/acsami.8b13550.

(S36) Wu, Z.; Yao, W.; London, A. E.; Azoulay, J. D.; Ng, T. N. Elucidating the Detectivity Limits in Shortwave Infrared Organic Photodiodes. *Adv. Funct. Mater.* **2018**, *28* (18), 1800391. https://doi.org/10.1002/adfm.201800391.

(S37) Biele, M.; Benavides, C. M.; Hürdler, J.; Tedde, S. F.; Brabec, C. J.; Schmidt, O. Spray-Coated Organic Photodetectors and Image Sensors with Silicon-Like Performance. *Adv. Mater. Technol.* **2019**, *4* (1), 1800158. https://doi.org/10.1002/admt.201800158.

(S38) Yoon, S.; Ryu, H. S.; Ha, J. U.; Kang, M.; Nguyen, T. L.; Woo, H. Y.; Chung, D. S. High-Performance Near-Infrared-Selective Thin Film Organic Photodiode Based on a Molecular Approach Targeted to Ideal Semiconductor Junctions. *J. Phys. Chem. Lett.* **2019**, *10* (18), 5647–5653. https://doi.org/10.1021/acs.jpclett.9b02481.

(S39) Joo, C. W.; Kim, J.; Moon, J.; Lee, K. M.; Pi, J.-E.; Kang, S.-Y.; Ahn, S.-D.; Park, Y.-S.; Chung, D. S. High-Performance Fab-Compatible Processed near-Infrared Organic Thin-Film Photodiode with 3.3×1012 Jones Detectivity and 80% External Quantum Efficiency. *Org. Electron.* **2019**, *70*, 101–106. https://doi.org/10.1016/j.orgel.2019.04.005.

(S40) Hassan, S. Z.; Cheon, H. J.; Choi, C.; Yoon, S.; Kang, M.; Cho, J.; Jang, Y. H.; Kwon, S.-K.; Chung, D. S.; Kim, Y.-H. Molecular Engineering of a Donor–Acceptor Polymer To Realize Single Band Absorption toward a Red-Selective Thin-Film Organic Photodiode. *ACS Appl. Mater. Interfaces* **2019**, *11* (31), 28106–28114. https://doi.org/10.1021/acsami.9b08326.

(S41) Lee, G. H.; Bulliard, X.; Bulliard, X.; Yun, S.; Leem, D.-S.; Park, K.-B.; Lee, K.-H.; Heo, C.-J.; Jung, I.-S.; Kim, J.-H.; Choi, Y. S.; Lim, S.-J.; Lim, S.-J.; Jin, Y. W.; Jin, Y. W. Green-Light-Selective Organic Photodiodes for Full-Color Imaging. *Opt. Express* **2019**, *27* (18), 25410–25419. https://doi.org/10.1364/OE.27.025410.

(S42) Xing, S.; Wang, X.; Guo, E.; Kleemann, H.; Leo, K. Organic Thin-Film Red-Light Photodiodes with Tunable Spectral Response Via Selective Exciton Activation. *ACS Appl. Mater. Interfaces* **2020**, *12* (11), 13061–13067. https://doi.org/10.1021/acsami.9b22058.

(S43) Strobel, N.; Droseros, N.; Köntges, W.; Seiberlich, M.; Pietsch, M.; Schlisske, S.; Lindheimer, F.; Schröder, R. R.; Lemmer, U.; Pfannmöller, M.; Banerji, N.; Hernandez-Sosa, G. Color-Selective Printed Organic Photodiodes for Filterless Multichannel Visible Light Communication. *Adv. Mater.* **2020**, *32* (12), 1908258. https://doi.org/10.1002/adma.201908258.

(S44) Opoku, H.; Bathula, C.; Shin, E.-S.; Long, D. X.; Kong, H.; Jung, Y. J.; Lim, B.; Noh, Y.-Y. Effect of Molecular Structure of Benzo[1,2-b:4,5-B′]Dithiophene-Based Push-Pull Type Donor Polymers on Performance Panchromatic Organic Photodiodes. *Org. Electron.* **2020**, *78*, 105580. https://doi.org/10.1016/j.orgel.2019.105580.

(S45) Liu, G.; Li, T.; Zhan, X.; Wu, H.; Cao, Y. High-Sensitivity Visible–Near Infrared Organic Photodetectors Based on Non-Fullerene Acceptors. *ACS Appl. Mater. Interfaces* **2020**, *12* (15), 17769–17775. https://doi.org/10.1021/acsami.0c00191.

(S46) Ko, H.; Park, S.; Son, H. J.; Chung, D. S. Wide-Linear-Dynamic-Range Polymer Photodiode with a New Benzo[1,2-b:4,5-B′]Dithiophene-Copolymer: The Role of Crystalline Orientation. *Chem. Mater.* **2020**, *32* (7), 3219–3228. https://doi.org/10.1021/acs.chemmater.0c00347.

(S47) Huang, J.; Lee, J.; Vollbrecht, J.; Brus, V. V.; Dixon, A. L.; Cao, D. X.; Zhu, Z.; Du, Z.; Wang, H.; Cho, K.; Bazan, G. C.; Nguyen, T.-Q. A High-Performance Solution-Processed Organic Photodetector for Near-Infrared Sensing. *Adv. Mater.* **2020**, *32* (1), 1906027. https://doi.org/10.1002/adma.201906027.

(S48) Dyson, M. J.; Verhage, M.; Ma, X.; Simone, G.; Tordera, D.; Janssen, R. A. J.; Gelinck, G. H. Color Determination from a Single Broadband Organic Photodiode. *Adv. Opt. Mater.* **2020**, *8* (7), 1901722. https://doi.org/10.1002/adom.201901722.

(S49) Bilgaiyan, A.; Elsamnah, F.; Ishidai, H.; Shim, C.-H.; Misran, M. A. B.; Adachi, C.; Hattori, R. Enhancing Small-Molecule Organic Photodetector Performance for Reflectance-Mode Photoplethysmography Sensor Applications. *ACS Appl. Electron. Mater.* **2020**, *2* (5), 1280–1288. https://doi.org/10.1021/acsaelm.0c00082.